Simulation of Orthocyclic Windings using the Linear Winding Technique

J. Bönig, B. Bickel, M. Spahr, C. Fischer and J. Franke

Institute for Factory Automation and Production Systems (FAPS),
Friedrich-Alexander-Universität Erlangen-Nürnberg (FAU)
Erlangen, Germany
Jochen.Boenig@faps.fau.de

***Abstract*— A continuously rising number of electric vehicle licensing is mentioned since the last few years in Germany. For a cost-efficient production of electrical engines in first-class quality and in sufficient quantity, it is indispensable to understand the process of coil winding. Thereby, the prediction of wire behavior is one of the key challenges. Therefore, a detailed model is built to investigate wire behavior during the linear winding process. The finite element based simulation tool LS-DYNA serves as explicit dynamics tool. The tool works with an explicit time integration method for time discretization. To represent the high dynamic process of winding within this simulation, dynamic influences such as rotational speed or acceleration of the coil body are definable. Within process simulation, the given boundary conditions are applied to the model. The non-linear material properties of the wire are validated under scrutiny by a tensile test and by values out of datasheets in previous research work. Simulation results of orthocyclic windings using the linear winding technique are presented within this paper. The dynamic simulation model is validated by experiments using the caster angle of the wire guide as reference parameter. The caster angel rises during the winding process of the first layer until the wire jumps to the next layer. Hence, it is possible to identify the maximum caster angle and match the simulation value against the experiment value. The travel profile of the wire guide is identified as extremely important to generate an orthocyclic winding. Another substantial part is the wire fixation respectively the geometry to support the first winding offset from winding one to winding two. Results of orthocyclic windings are simulated with and without grooves on the coil body surface and demonstrate the positive influence of grooves for an accurate orthocyclic winding picture.**

Keywords—Explicit dynamics, simulation, linear winding

I. INTRODUCTION

The stringent necessity to simulate the winding process is caused by the lack of process knowledge and the possibility to increase the copper fill factor during machine design phase [1]. Looking at the linear winding technique seems to be the correct first step in winding simulation, since linear winding is a highly productive process and kind of simple compared to other winding techniques, like needle or flyer winding process. Other research approaches [2] focus also on the linear winding process. Despite the ascending complexity of winding schemes for electric drives, single-tooth winding scheme is state of the art in automotive industry [3].

One resulting challenge is the simulation of several layers while considering the correct deformation behavior of the wire during the process. The highly nonlinear winding process includes all kinds of nonlinearities. Geometric nonlinearity occurs because of the large wire deformations. Material nonlinearity crops up based on the elastic-plastic material properties of the copper wire. Structural nonlinearity exists via the non-linear contact behavior between wire and coil body and the wire self-contact including friction. Additionally, the process is transient and, therefore, supplementary time-consuming to simulate.

The need for research is consequently a simulation model dealing with the non-linear process, exact deformation condition, and the high number of windings. Therefore, the simulation time is identified as critical factor. Using the simulation, the process has to be investigated to optimize the winding result for the given boundary conditions. The identified influence factors for a winding result from former research [4] and specify the parameters to be investigated.

The approach is, to solve this challenges by the explicit dynamic simulation using LS-DYNA solver [4]. Here, the computational cost is reasonable compared to an implicit time integration method. The model is validated via experiments by the caster angle of the wire guide. Therefore, experimental results from former research [5] are used. This dynamic and validated model is applied to investigate the influence parameters wire fixation, grooves, caster angle, rotational speed and wire guide traversing profile.

II. SIMULATION MODEL

The pre-processing is realized in ANSYS Workbench. The chosen solver for computing the winding process is LS-DYNA. For the post-processing LS-PrePost, ANSYS Workbench and Matlab are applied. The model consists of three bodies. Coil body and winding guide are represented by rigid bodies. The copper wire is modeled flexibly with a multi-linear stress-strain curve, to get best fit referring to the elastic-plastic material behavior.

978-1-4673-7512-2/15/$31.00 ©2015 IEEE

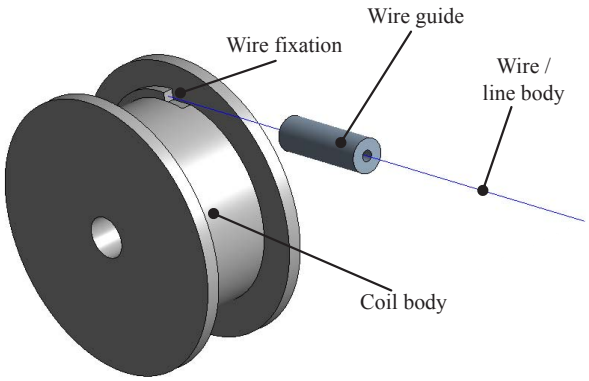

Fig. 1. Geometry model of the linear winding process

Wire guide and coil body are designed as solid bodies and the wire as line body. The cross section of the wire is defined round and has a diameter of 1.6 mm. The wire fixation on the coil body is designed as a chock and represents an optimization parameter. The round coil body has a diameter of 30 mm. The rigid bodies are meshed with constant stress solid elements. The wire discretization is done with Hughes-Liu beam elements. These beam elements support the multi-linear material behavior. We set the element length to 2.0 mm. The element length influences directly the simulation time via the courant friedrich levy number [4] and is optimized referring to calculation time and result accuracy. For a proper definition of the model, four contacts must be defined during pre-processing. We have a bonded contact between coil body and wire fixation. This contact type is called TIED_NODES_TO_SURFACE. The friction effected contact between wire and coil body is modeled via the AUTOMATIC_BEAMS_TO_SURFACE contact type, as well as the contact between wire and wire guide. Furthermore, the beam self-contact uses the AUTOMATIC_GENERAL contact typ. The coefficient of friction is 0.1 and caused by the coating layer of the copper wire. Boundary conditions and loads are defined in ANSYS Workbench. The displacement of the wire guide A, the wire pull force B and the displacement of the coil body C are visualized in Fig. 2. The wire pull force in this study, for example, is constant 50 N and is located in the midrange referred to a maximum permissible force of 100 N. The maximum wire pull force depends on wire diameter and material [4]. The rigid body rotations allow the variation of winding speed and acceleration. The displacement of the wire guide enables us to configure the traversing profile. The load at the end of the wire represents the wire pull force.

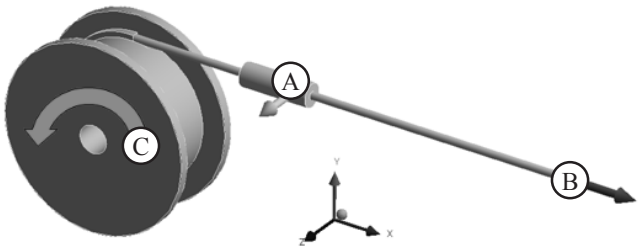

Fig. 2. Boundary conditions of the simulation model

III. VALIDATION OF THE DYNAMIC PROCESS

The simulation in LS-DYNA is validated with experimental results of [5]. The validation is based on the maximum caster angle α_{max}. The definition of the caster angle α is visualized in Fig. 3. The caster angle is positive, if the wire guide lags and negative for a leading wire guide.

A negative caster angle affects a disadvantageous winding result [5]. The angle α_{max} appears when the wire starts to take off from the coil body and deposits on the wound layers. For the given boundary conditions of a 30 mm coil body diameter d_c and wire diameter d_w of 1.6 mm, results the determined empirically formula:

$$\alpha_{max} = 11.89° + 3.41° \cdot \ln\left(\frac{d_w}{mm}\right) = 13.37° \tag{1}$$

Additionally, Dobroschke [5] developed an analytical equation to calculate the positive α_{max} for round coil bodies depending on d_c and d_w:

$$\alpha_{max} = 51.52° \cdot \left(\frac{d_c}{mm}\right)^{-0,41} + 11.31° \cdot \left(\frac{d_c}{mm}\right)^{-0,33} \cdot \cdot \ln\left(\frac{d_w}{mm}\right) = 14.51° \tag{2}$$

Dobroschke [5] recommends a target caster angle α_t for an optimal winding result, that depends on α_{max} and a safety factor S. The value of the safety factor is 0.4. The target angle is the product of maximum caster angle α_{max} and safety factor S:

$$\alpha_t = S \cdot \alpha_{max} = 0.4 \cdot 14.51° = 5.8° \tag{3}$$

The validation via the parameter α_{max} needs a simulation study. The performed simulation is shown in Fig. 4. Step 1 illustrates the initial state of the simulation study. Step 2 serves as preparation of the neutral winding picture. In Step 3, the stop of the wire guide and continuing winding process with rising caster angle is shown. Thereby, the caster angle increases by a value of 1.41° per rotation. Step 4 pictures the accumulation of the current winding to the already placed former windings. The maximum caster angle is determined in LS-PrePost. The resolution in post-processing amounts 106 pictures per rotation.

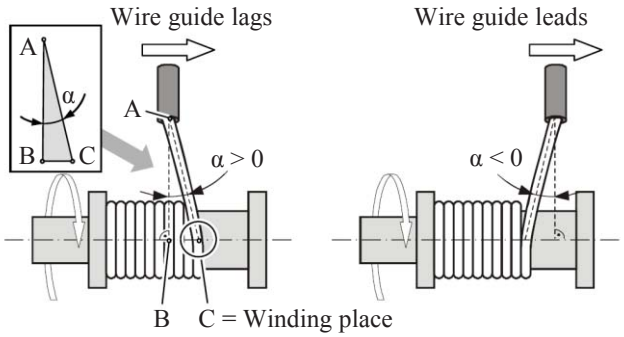

Fig. 3. Definition of the caster angle [5]

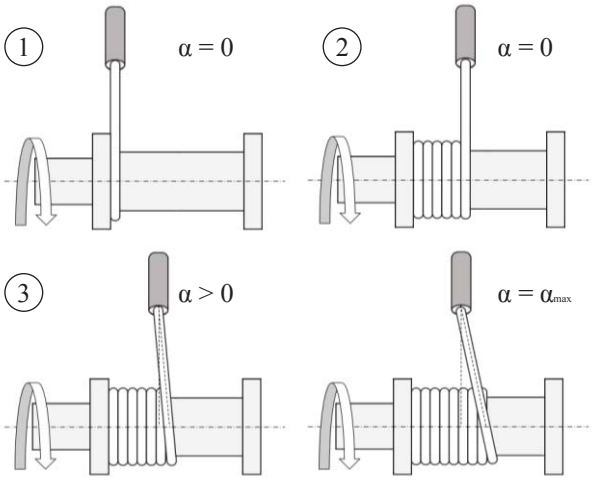

Fig. 4. Sequence of the caster-angle determination

The simulation study leads to a maximum caster angle of 13.15° and is comparable to the empirically result of Dobroschke [5].

In addition, wire stresses are simulated correctly. The normal stress curve shows a rising at the clamping (wire fixation), which is provable via rope friction. The normal stress at the winding place is definable by an analytical calculation [6] and depends on the wire pull force F_t and the wire cross sectional area A_w:

$$\sigma_t = \frac{F_t}{A_w} = \frac{50\,\mathrm{N}}{2.01\,\mathrm{mm}^2} = 24.9\,\frac{\mathrm{N}}{\mathrm{mm}^2} \tag{4}$$

Using the approach of rope friction, the necessary tensile force of the coil body F_{cb} at the clamping is calculated by the following equation [7]:

$$F_{cb} = F_t \cdot e^{\mu\cdot\alpha} = 50\,\mathrm{N} \cdot e^{0.01\,\cdot\,18.8\,\mathrm{rad}} = 60.34\,\mathrm{N} \tag{5}$$

The normal stress including the rope friction at the clamping results:

$$\sigma_{tcb} = \frac{F_{cb}}{A_w} = \frac{60.34\,\mathrm{N}}{2.01\,\mathrm{mm}^2} = 30.04\,\frac{\mathrm{N}}{\mathrm{mm}^2} \tag{6}$$

The analytical results equal the simulated maximum and minimum normal stresses (see Fig. 5). Besides the normal stress, the bending stress is also pictured in Fig. 5. We affiliate the lower value at the clamping to the displacement boundary condition.

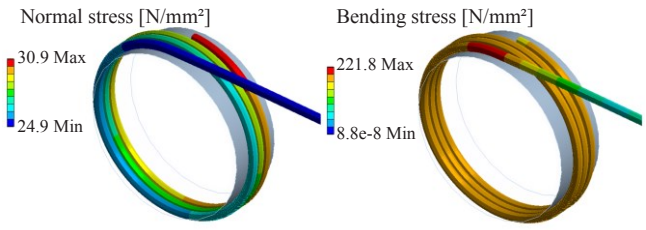

Fig. 5. Normal (left) and bending stress (right) of the copper wire

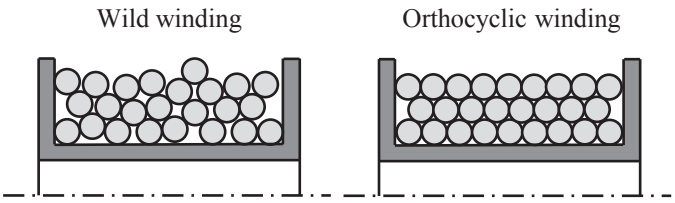

Fig. 6. Difference between wild and orthocyclic winding picture [9]

IV. Simulation of Orthocyclic Windings

The key challenge in coil winding is to achieve the highest possible mechanical fill factor k_m. The value for wild windings is $k_m \approx 0.65\text{-}0.75$ % and for orthocyclic windings $k_m = 0.907$ % (cf. Fig. 6) [8]. Hence, an orthocyclic winding picture yields better results with relation to the efficiency.

Windings are winded parallel to the side panel to generate an orthocyclic winding picture. Therefore, a phase shift is needed, otherwise a helix results and the layers cross each other. The windings of a second layer would not lie between the windings of the first layer and prevents the strived honeycomb structure. Winding with phase shift, however, enables a placing of new windings between the windings of former layers and, thus, a higher fill factor arises. Crossing windings result only in the area of phase shift. To support a harmonic phase shift the clamping of the wire is design like a chock (cf. Fig. 7). The chock wields the translational displacement of the wire along the coil body axis. To investigate the chock design, the phase shift is simulated with three different chock lengths l_c (cf. Fig. 7). The chosen chock lengths depends on the wire diameter d_w. The presented results are based on chocks with lengths of $l_c = 3d_w$, $l_c = 6d_w$ and $l_c = 9d_w$ (from the left to the right).

The smoothest phase shift results for the longest chock length. The wire is in contact with the former winding and yields the best results. The following examinations are performed with the described configuration.

The former validation via the maximum caster angle is based on a continuous winding process without phase shift. Hence, the caster angle for windings including phase shift needs to be checked in the simulation model. The start parameters include a caster angle of 5° and a rotational speed of 2000 rpm. The coil-body diameter of 30 mm and the wire diameter of 1.6 mm persist during investigations.

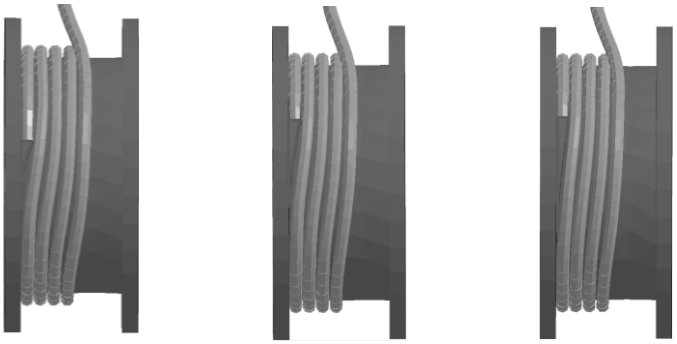

Fig. 7. Chock design to support the phase shift

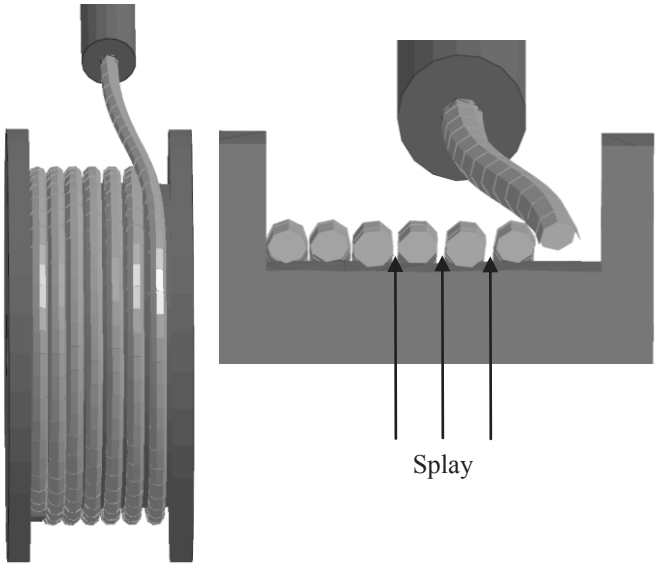

Fig. 8. Resulting splay for a caster angle of 5°

The resulting winding picture shows a splay of windings. An increasing splay is detected after the third winding (cf. Fig. 8). In addition, a change of the rotational speed yields also to splays. Hence, a separate study of the optimum caster angle for windings including phase shifts is started. The winding process is simulated for 500, 1000 and 2000 rpm. Independently of rotational speed, the optimum caster angle is at 2° in our configuration.

Figure 9 shows the nominal-actual comparison for the first six windings depending on the caster angle. The rotational speed is 500 rpm. The seventh winding could get in contact with the coil body wall, push the former windings back and falsify the result.

The sixth winding with a caster angle of 7° has a deviation to the target place of nearly one wire diameter (cf. Fig. 9). This is not acceptable for winding processes. The seventh winding overleaps which results to a wild winding. With the 2° caster angle, it is possible to place eight windings parallel in layer one. The last winding pushes the former ones aside and forces in the leftover gap. Hence, the orthocyclic winding is feasible but not perfectly accurate.

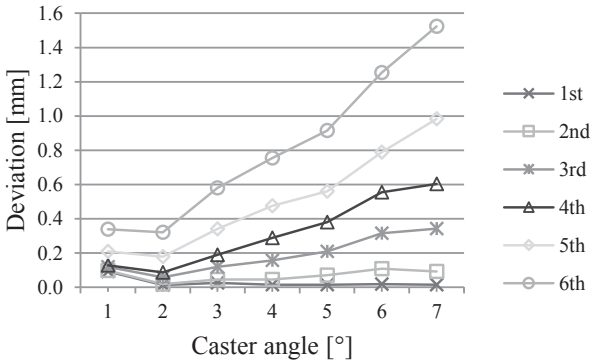

Fig. 9. Deviation to the target position depending on the caster angle

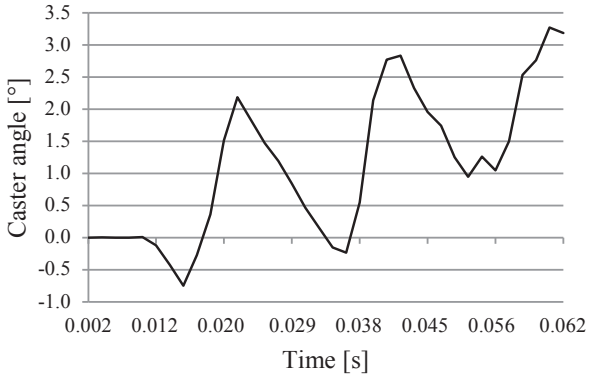

Fig. 10. Picture detail of the simulated caster angle profile over the time by a nominal caster angle of 2°

The winding behavior is caused by the continuously changing caster angle during the process. Compared to the continuous winding process, the winding with defined phase shift leads, during a linear displacement of the wire guide, to an oscillating caster angle (cf. Fig. 10). The wire guide traversing profile does not consider the phase shifts during the winding process. Thus, the target caster angle oscillates strongly because of the high wire diameter and the resulting abrupt phase shift of 1.6 mm (cf. Fig. 11). The defined wire guide traversing profile leads to caster angles up to 5° and even negative values. In reality, the caster angle changes additionally by the splay between the windings but the major influence factor is the abrupt phase shift.

The optimization of the wire guide traversing profile presents future work. The developed theoretical approach involves a negative displacement of the wire guide before the winding process starts, to compensate the negative caster angle at the beginning. In addition, the rising caster angle will be compensated via faster displacements of the wire guide during the phase shifts (cf. Fig. 12). The realization of the theoretical wire guide displacement will be investigated in upcoming studies and depends on the technical feasibility of the winding machine.

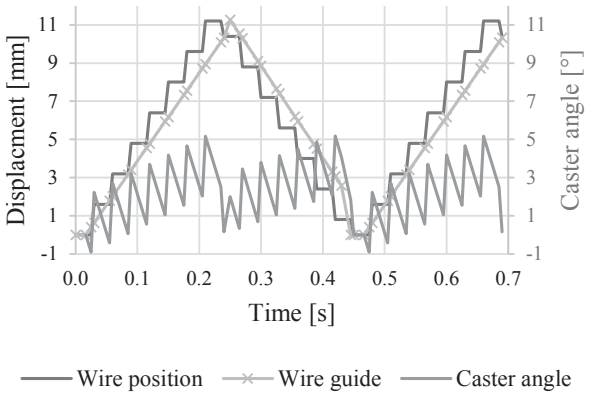

Fig. 11. Theoretical caster angle profil depending on the wire guide traversing profile and the target position of the wire at the winding place

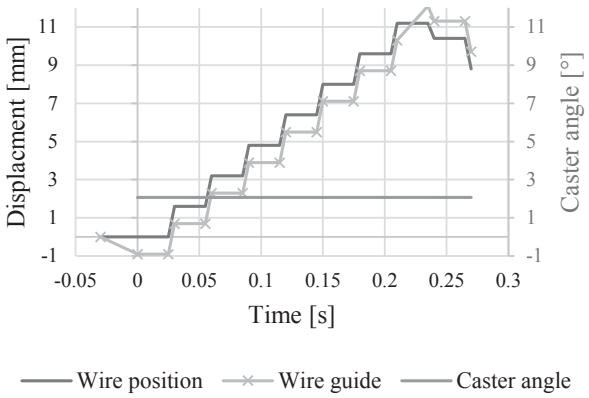

Fig. 12. Constant caster angle caused by the theoretical wire guide traversing profile

Nevertheless, an approximation to the target profile is realistic and small fluctuations of the caster angle are acceptable and can be compensated.

Another common approach to generate an accurate first winding layer is a design optimization of the coil body via grooves on the winding surface (cf. Fig. 13). The first winding layer is the decisive influence factor for a controlled layer structure since windings of the first layer specify the placing for the windings of the second layer. The grooves on the coil body surface have a depth of 0.2 mm in our coil body design and are discontinuous at the area of the enforced phase shift.

The windings of the first layer cling to the grooves and get their defined position supported by the wire pull force and the fitting radii (regarding the wire diameter). The evaluation of the simulation results of the coil body is illustrated in Fig. 14. The deviation of the first four windings depends on the caster angle. It yields to a maximum deviation of 0.011 mm at the fourth winding and a caster angle of 7°.

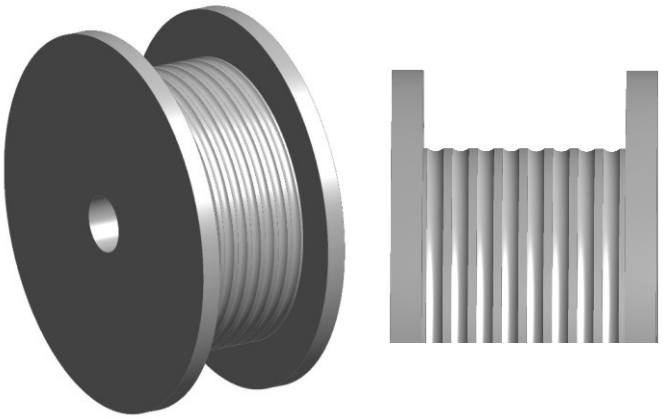

Fig. 13. Round coil body with grooves on the winding surface

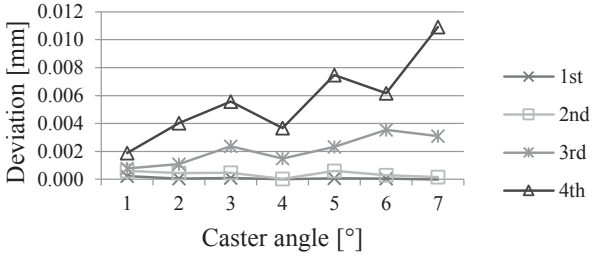

Fig. 14. Deviation to the target position depending on the caster angle for coil body with grooves on the winding surface

The deviation of the windings in relation to the target position is 100 times more accurate than without grooves. Despite the changing caster angle, the support of the grooves compensates the splay. The first two windings are independent from the increasing caster angle. Only starting from the third layer, the deviation increases with the caster angle. The prerequisite for a positionally accurate structure is provided via grooves on the winding surface. Figure 15 visualizes the simulated winding result and the target honeycomb winding structure.

The layer accuracy demonstrates only small horizontal deviations in comparison to the perfect winding result. The rough meshing of the coil body leads to a constant deviation of 0.075 mm in vertical direction (cf. Fig. 16). The radial deviation of the windings is continuous about 0.1 mm except the seventh winding of the third layer. Here, the deviation rises to 0.2 mm. This testifies an accurate winding result while considering the constant deviation caused by the rough mesh of the coil body.

Dobroschke‘s [5] endorsed target angle for a continuous winding is not directly transferable to an orthocyclic winding. Despite a predefined guidance of windings via chock, splays result during layer structuring caused by phase shift. Satisfying simulation results occur only by optimizing the coil body via grooves on the winding surface. The grooves are the prerequisite for an orthocyclic winding.

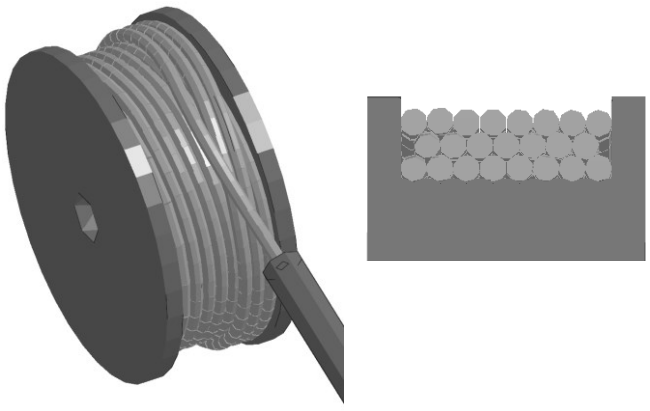

Fig. 15. Orthocyclic winding picture with three layers and the strived honeycomb structure

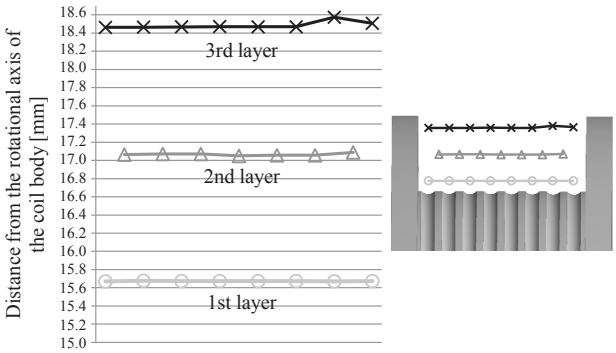

Fig. 16. Detailed layer structre of an orthocyclic winding supported via grooves on the winding surface

V. Summary and future Work

Mentioned at the beginning, the motivation is a better understanding of the winding process and a possibility to predict wire behavior via simulation. The presented approach is able to simulate realistic wire behavior. In addition, new insights regarding the linear winding process are published. In detail, a simulation-based optimization to an orthocyclic winding for round coil bodies is showcased. To simulate three layers, the LS-DYNA solver computes about eight hours for a rotational speed of 2000 rpm. Hence, the simulation model is a suitable tool to investigate the linear winding process.

First, a description of the pre-processing settings are carried out to define the boundary conditions of the simulation model. With this, material properties, geometry, contact behavior, meshing, boundary conditions, and other analysis settings are defined. Hence, the simulation model specification is concluded and ready for parameter studies.

Second, the validation of the dynamic winding process is carried out via the maximum caster angle experiments of Dobroschke [5]. Additionally, the resulting stresses of the simulation are validated by analytic calculations. The validation via experiments and analytical calculations yields to an agreement of results. In addition to [1], [2], and [4], a dynamic validation of the simulation model is presented.

Third, the simulation study to generate orthocyclic windings is performed by the validated model. The first approach is based on chock designs to support the phase shift of the windings. The constant wire guide traversing profile leads to an oscillating caster angle and splays between the windings. Further, the target caster angle for constant winding does not work for orthocyclic winding with phase shift. The second approach focuses on coil body optimization by grooves on the winding surface. The coil body optimization works and the strived honeycomb structure results accurately.

This work focuses the investigation of the presented concept on two selected influence quantities of Bönig et al [4], the remaining parameters present future work. A particular problem therein is the wire guide traversing profile. Adaptions to the displacement behavior of the wire guide will be presented in future work, too. A first theoretical approach is described in this paper.

The identified influence quantities [4] depend mostly on each other. The resulting high number of influence factors leads to complex further research in the field of linear coil winding. The simulation is a common approach to support scientific work, e.g. in metal forming. Hence, the developed simulation model will be used and updated for future investigations concerning winding processes.

VI. References

[1] J. Bönig, B. Bickel, M. Ebenhöch, M. Spahr, C. Fischer, and J. Franke, “Structural mechanics process simulation of linear coil winding,” in *WGP Congress 2014: Progress in Production Engineering*, Switzerland: Trans Tech Publications, 2014, pp. 47–54.

[2] F. S.-L. Blanc, E. Ruprecht, and J. Fleischer, “Material based process model for linear noncircular coil winding processes with large wire gauge: Investigation of wire material influences on the winding process and compensation approaches,” in *3rd International Electric Drives Production Conference: Proceedings*, Piscataway, NJ: IEEE Service Center, 2013, pp. 128–132.

[3] J. Bönig, C. Fischer, V. Marquardt, S. Matzka, and J. Franke, “Methodical Integration of Assembly Specific Influences concerning High-Voltage Components into the Virtual Validation Process,” in *2nd International Electric Drives Production Conference: Proceedings*, Piscataway, NJ: IEEE Service Center, 2012, pp. 101–108.

[4] J. Bönig, B. Bickel, M. Spahr, C. Fischer, and J. Franke, “Explicit Dynamics Process Simulation of Linear Coil Winding for Electric Drives Production,” in *4th International Electric Drives Production Conference: Proceedings*, Piscataway, NJ: IEEE Service Center, 2014, pp. 210–216.

[5] A. Dobroschke, *Flexible Automatisierungslösungen für die Fertigung wickeltechnischer Produkte*. Bamberg: Meisenbach Verlag, 2011.

[6] H. Dubbel, W. Beitz, and K.-H. Grote, *Taschenbuch für den Maschinenbau,* 20th ed. Berlin [u.a.]: Springer, 2001.

[7] A. Böge, *Technische Mechanik: Statik - Dynamik - Fluidmechanik - Festigkeitslehre,* 28th ed. Wiesbaden: Vieweg + Teubner, 2009.

[8] K.-U. Wolf, *Verbesserte Prozessführung und Prozessplanung zur Leistungs- und Qualitätssteigerung beim Spulenwickeln*. Bamberg: Meisenbach, 1997.

[9] M. Camardella and T. A. Manning, “Winding Perfect Layer Coils,” in *1989 coil winding proceedings: September 25-28, 1989*, Minneapolis, MN: International Coil Winding Association, 1989, pp. 108–113.